Indonesian Journal of Science & Technology

Journal homepage: http://ejournal.upi.edu/index.php/ijost/

High-Porosity Hydrochar From Oil Palm Empty Fruit Bunches Via Single-Step Hydrolytic Agent-Assisted Hydrothermal Carbonization

Wanchana Sisuthog[1], Natthawan Prasongthum[2], Amornrat Suemanotham[2], Yoothana Thanmongkhon[2], Lalita Attanatho[2], Sasiradee Jantasee[1], Weerinda Mens[1], Chaiyan Chaiya[1,]*

[1]Rajamangala University of Technology Thanyaburi, Pathum Thani, 12110, Thailand
[2]Thailand Institute of Scientific and Technological Research (TISTR), Pathum Thani, 12120, Thailand
*Correspondence: E-mail: chaiyan_c@rmutt.ac.th

ABSTRACT

Empty fruit bunches (EFBs) discarded from the palm oil industry were converted into hydrochars with a high surface area via hydrolytic agent-assisted hydrothermal carbonization (HTC). The reaction temperature was varied (160, 200, 240, and 280 °C) for a constant reaction time of 2 h. The effects of the type of hydrolytic agent (H_2O_2 and H_2SO_4) on the hydrochar properties were investigated. The physical and chemical properties of the as-obtained hydrochars, such as surface area, porosity, morphology, functional groups, and elemental composition, were characterized. The results showed that the fixed carbon and carbon contents increased with increasing temperature. At 280 °C, the hydrochar produced via the H_2SO_4-assisted HTC process had the highest fixed carbon (38.35 wt.%) and carbon (72.65 wt.%) contents. In comparison, the hydrochar (O-EFB280h2) produced via the H_2O_2-assisted HTC process at 280 °C exhibited the highest surface area (479.19 m^2/g) and pore volume (0.727 cm^3/g), and it contained functional groups such as C-H, C=O, and C-O. The H_2O_2-assisted HTC process produced hydrochars with a high surface area that could be used in a variety of applications.

ARTICLE INFO

Article History:
Submitted/Received 29 May 2024
First Revised 02 Jul 2024
Accepted 06 Sep 2024
First Available Online 07 Sep 2024
Publication Date 01 Dec 2024

Keyword:
Empty fruit bunches,
Hydrochar,
Hydrolytic agent,
Hydrothermal carbonization.

1. INTRODUCTION

Thailand's oil palm industry has expanded rapidly owing to extensive oil palm cultivation. Empty fruit bunches (EFBs) are solid wastes generated during palm oil manufacturing. Converting EFBs into higher value-added products using thermochemical processes, such as pyrolysis, carbonization, activation, gasification, or hydrothermal carbonization (HTC), is an interesting alternative. These processes generally yield solid or liquid carbon materials (Mamimin *et al*., 2021; Puccini *et al*., 2017; Rohimi *et al*., 2022; Soha *et al*., 2021; Wadchasit *et al*., 2021; Yan *et al*., 2019). However, HTC is a compatible process with high-moisture-content materials such as EFBs. Water molecules in EFBs may be beneficial for the HTC process because the HTC reaction occurs between the raw material and water at high pressures. These conditions result in subcritical water. The acidic or basic ionic properties of subcritical water enhance the reactivity of processes such as hydrolysis. These characteristics of subcritical water facilitate the breakdown of biomass during hydrothermal processes (Cebi *et al*., 2022; R. Li & Shahbazi, 2015; Wu *et al*., 2023a). However, the HTC process cannot produce materials with a high porosity. According to Li (F. Li *et al*., 2020) and R. (Khoshbouy *et al*., 2019), the surface areas of hydrochars produced via HTC were in the range of 1.7–6.3 m^2/g.

Roman *et al*. (2013) prepared a hydrochar from walnut shells with a low surface area of 31 m^2/g. A few years ago, the application of hydrolytic agents as activators was the preferred method for increasing the surface area of a hydrochar. The addition of activators to the HTC process accelerated both hydrolysis and dehydration, which occurred in a single step at lower temperatures, as well as the development of chemical functional groups, and also increased porosity (Malaika *et al*., 2020). This is advantageous for hydrochars used in catalysis or adsorption processes involving porous materials. Nizamuddin *et al*. (2017) investigated the effect of the addition of RbOH and CsOH (basic activators) on hydrochar production from pine wood via HTC and found that the amount of the liquid product increased, whereas that of the solid product decreased. The use of an acidic H_2SO_4 activator during the HTC process produced uniformly porous hydrochars (Zhang *et al*., 2021). The use of H_2O_2 as an activator increased both the number of oxygenated functional groups (OFGs) and the porosity of the hydrochar (Jain *et al*., 2015). K_2CO_3 was proven to be an effective basic activator for sawdust conversion into hydrochar. It is thermally stable, effective, and cost-efficient, with a high selectivity toward the desired product, thereby increasing the product yield (Duy Nguyen *et al*., 2019).

Therefore, the purpose of this study was to convert EFBs obtained from the palm oil industry into hydrochars with a high surface area in a single step using HTC and hydrolytic agents. The effects of various hydrolytic agents (H_2SO_4 and H_2O_2) and operating temperatures (160, 200, 240, and 280 °C) were investigated (Kambo & Dutta, 2015; R. Li & Shahbazi, 2015). Physical parameters such as the surface area and morphology, and chemical variables such as the functional groups and elemental composition, were determined. Furthermore, for each hydrolytic agent, a Van Krevelen diagram was plotted to predict the chemical pathways occurring during the HTC process. This study aims to produce highly porous hydrochars that can be used in processes that require the material to have a large surface area and contain some chemical functional groups, such as reaction catalysis or adsorption processes.

DOI: https://doi.org/10.17509/ijost.v9i3.74551
p- ISSN 2528-1410 e- ISSN 2527-8045

2. METHODS

2.1. Raw Materials

EFBs sourced from the palm oil industry in Thailand were used as primary raw materials. They were subjected to a drying process in an oven for an extended period at a temperature of 105 °C and then fragmented into smaller particles using a mechanical crusher. Before the hydrothermal process, they were subjected to a mechanical sieving procedure using a sieve with a maximum aperture size of 2 cm.

2.2. HTC Process

The HTC process was performed in a 4.5-L high-pressure batch reactor outfitted with an automatic stirrer and a controllable electric heater. Hydrolytic solutions of 0.1 M H_2SO_4 and 0.1 M H_2O_2 were prepared. In the HTC process, 100 g of EFBs was mixed with 1,000 g of the hydrolytic solution (mass ratio = 1:10) in the reactor, which was then filled with N_2 gas until the pressure reached 20 bar and the gas was released. The gas-filling process was repeated until all remaining air was removed. The reaction temperature was varied (160, 200, 240, and 280 °C) for a constant reaction time of 2 h under N_2 atmosphere, after which the reactor was cooled to room temperature and the product was collected. The solid and liquid phases of the product were separated by vacuum filtration. The solid-phase product was dried in an oven at 105 °C for 24 h before storing it in a moisture-free vessel. The experimental setup is shown in **Figure 1**. In this study, the HTC-treated hydrochars activated using H_2SO_4 were labeled as A-EFB, whereas those activated using H_2O_2 were labeled as O-EFB.

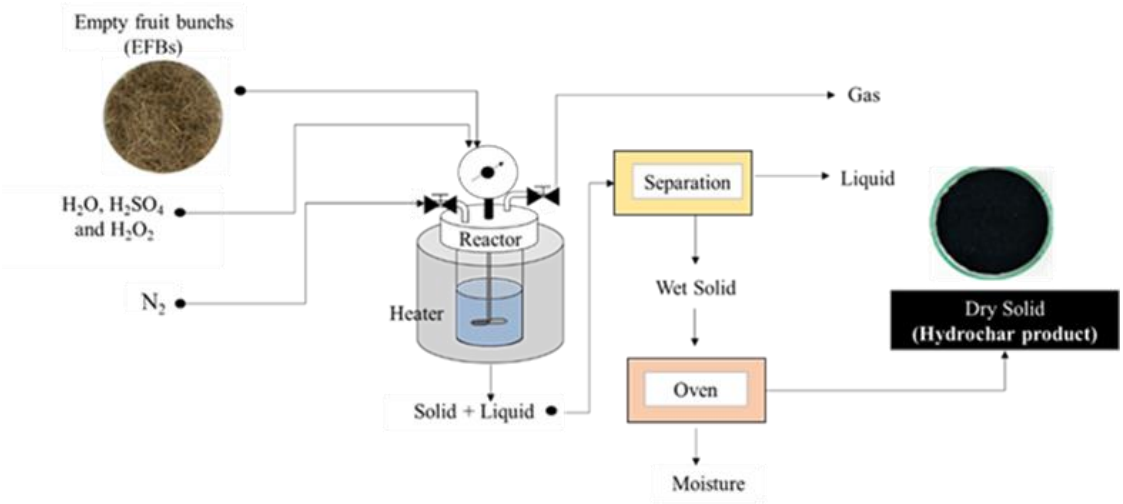

Figure 1. Schematic diagram of the HTC process.

2.3. Characterization

The as-prepared hydrochars were weighed and collected to analyze the product yields. Ultimate analysis was performed using a CHNS analyzer to determine the carbon, hydrogen, nitrogen, and oxygen contents following the ASTM D5373 and ASTM D4239 standards. Proximate analysis was performed according to the ASTM D7582 standard. An automated gas adsorption analyzer (Quantachrome Autosorb IQ Station 1, USA) was used to determine the surface area, pore size, and pore volume. The surface morphology was analyzed using scanning electron microscopy (SEM, JEOL JSM 7800F, Japan). The chemical functional groups in the biochars were identified using Fourier-transform infrared spectrometry (FTIR, Shimadzu model IRresting-21, Japan).

DOI: https://doi.org/10.17509/ijost.v9i3.74551
p- ISSN 2528-1410 e- ISSN 2527-8045

3. RESULTS AND DISCUSSION

3.1. Proximate and Ultimate Analyses

The major components of raw EFBs and all hydrochars were analyzed using proximate and ultimate analyses, as shown in **Tables 1** and **2**. The results revealed that the hydrochar yield decreased with increasing hydrothermal temperature. Although, the highest biochar yields were obtained at 160 °C, their textures were still brown, which indicated that the cellulose in the O-EFB160h2 and A-EFB160h2 samples was not completely decomposed. This is because cellulose typically decomposes at temperatures above 200 °C. At temperatures of 160 and 200 °C, the hydrochars catalyzed using H_2O_2 exhibited higher yields than those catalyzed using H_2SO_4. Interestingly, the yield of the hydrochars catalyzed using H_2O_2 decreased from 39.00 to 34.24 wt.% at temperatures above 200 °C, while keeping the composition and fixed carbon content constant. This may be attributed to the extreme structural changes occurring between 240 and 280 °C under H_2O_2 activation. The fixed carbon and carbon contents are essential parameters for evaluating the performance of carbon materials. The A-EFB280h2 sample had the highest fixed carbon (38.35 wt.%) and carbon (72.65 wt.%) contents. Its fixed carbon content was approximately 2.7 times that of the EFBs. The volatile matter content of the EFBs was high (73.82 wt.%). The increase in fixed carbon content after the hydrothermal carbonization process is due to the removal of oxygen and hydrogen, the formation of aromatic carbon structures, the loss of volatile compounds, and the carbonization of biomass. These changes result in a solid product with a higher carbon content and better fuel properties (Wu *et al*., 2023b) compared to the original biomass.

Table 1. Proximate analysis data.

Samples	Yield (%)	Proximate analysis (% dry basis)			
		Moisture	Volatile matter	Fixed carbon	Ash
EFBs	-	5.97 ± 0.10	73.82 ± 1.00	14.35 ± 0.09	5.86 ± 0.99
A-EFB160h2	51.96	2.98 ± 0.01	78.57 ± 1.70	15.34 ± 0.33	3.12 ± 0.06
A-EFB200h2	43.80	2.78 ± 0.01	65.21 ± 1.34	28.20 ± 0.57	3.81 ± 0.08
A-EFB240h2	40.72	2.36 ± 0.01	61.40 ± 1.05	32.75 ± 0.56	3.50 ± 0.06
A-EFB280h2	42.63	2.33 ± 0.01	54.23 ± 0.92	38.35 ± 0.52	5.09 ± 0.08
O-EFB160h2	64.71	3.98 ± 0.01	84.11 ± 2.46	10.25 ± 0.30	1.67 ± 0.04
O-EFB200h2	56.31	2.91 ± 0.06	79.24 ± 1.68	15.21 ± 0.33	2.64 ± 0.06
O-EFB240h2	39.00	1.76 ± 0.01	63.72 ± 0.81	30.54 ± 0.39	3.98 ± 0.05
O-EFB280h2	34.24	1.44 ± 0.01	62.71 ± 0.66	30.97 ± 0.32	4.88 ± 0.06

Table 2. Ultimate analysis data.

Samples	Ultimate Analysis (% dry basis)			
	H	C	N	O
EFBs	6.34 ± 0.05	50.49 ± 0.38	0.78 ± 0.07	36.05 ± 0.31
A-EFB160h2	6.68 ± 0.09	56.23 ± 1.18	0.23 ± 0.00	32.98 ± 1.18
A-EFB200h2	6.30 ± 0.10	68.71 ± 1.35	0.36 ± 0.01	20.02 ± 1.35
A-EFB240h2	6.31 ± 0.08	71.38 ± 1.19	0.38 ± 0.01	17.63 ± 1.19
A-EFB280h2	5.88 ± 0.08	72.65 ± 1.20	0.33 ± 0.01	15.15 ± 1.22
O-EFB160h2	6.58 ± 0.13	53.67 ± 1.51	0.00 ± 0.00	37.94 ± 1.43
O-EFB200h2	6.57 ± 0.09	57.20 ± 1.17	0.12 ± 0.05	33.24 ± 1.15
O-EFB240h2	6.56 ± 0.06	69.68 ± 0.87	0.64 ± 0.01	18.86 ± 0.87
O-EFB280h2	6.80 ± 0.05	71.36 ± 0.73	0.82 ± 0.01	15.87 ± 0.75

DOI: https://doi.org/10.17509/ijost.v9i3.74551
p- ISSN 2528-1410 e- ISSN 2527-8045

According to the results of the ultimate analysis, the hydrogen content of all biochars remained relatively constant, whereas the oxygen content decreased with increasing HTC temperature. Carbon, hydrogen, and oxygen contents are the key factors for predicting the reaction steps in the HTC process using the Van Krevelen diagram (Ameen *et al*., 2022). As shown in **Figure 2**, the Van Krevelen diagram was plotted for the atomic ratios of H/C and O/C of the EFBs and produced hydrochars. Each diagram represents the results of hydrochars catalyzed by hydrolytic agents and the non-catalyzed hydrochars prepared in our previous study (Zhu *et al*., 2022). When the HTC temperature was increased from 160 to 280 °C, the H/C and O/C ratios of the H_2SO_4-catalyzed hydrochars decreased to 0.96 and 0.15, respectively. Their Van Krevelen trend line matched that of the non-catalyzed hydrochars (**Figure 2a**). Only the dehydration reaction occurred over the entire HTC temperature range when H_2SO_4 was used. As shown in **Figure 2b**, the H/C and O/C ratios of the hydrochars catalyzed by H_2O_2 decreased with increasing HTC temperature. However, the chemical route was temperature-dependent when H_2O_2 was used. Dehydration occurred when the HTC temperature ranged from 160 to 240 °C, whereas decarboxylation occurred when the temperature exceeded 240 °C (Fakkaew *et al*., 2015). Decarboxylation is the reaction in which the carboxyl group [−C(O)OH] from the cellulose molecule is replaced by a hydrogen atom, resulting in the emission of the corresponding alkane (R-H) and carbon dioxide (CO_2). Decarboxylation occurs in thermochemical processes such as carbonization, pyrolysis, or HTC. However, the effect of decarboxylation on the porosity was more evident in the BET results.

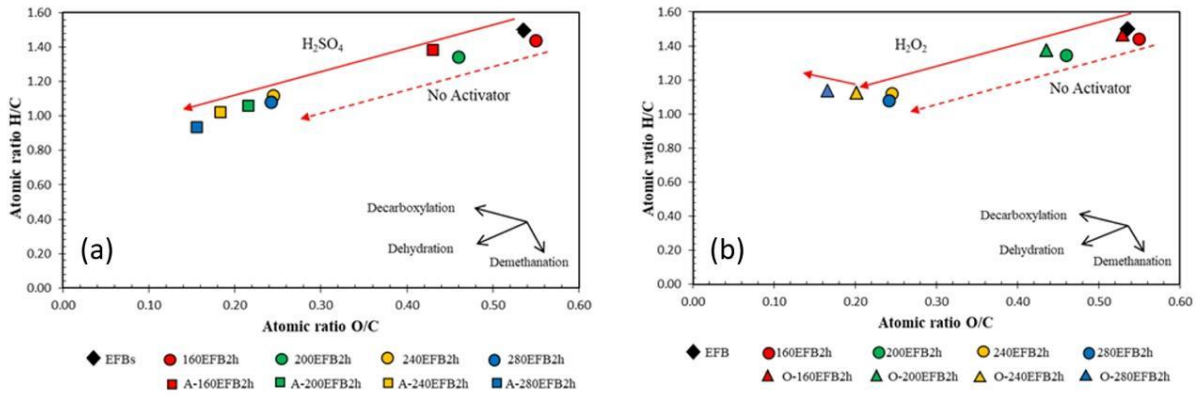

Figure 2. Van Krevelen diagram of the EFBs, non-activated hydrochars, and activated hydrochars under chemicals: (a) H_2SO_4 (b) H_2O_2.

3.2. BET and SEM Analyses

The N_2 adsorption data of hydrochars were adjusted for structural type analysis. As shown in **Figures 3** and **4**, the porosity of hydrochars was defined as the ratio of the volume of the pores and voids to the volume occupied by the solid. Porous materials are also defined in terms of their adsorption properties. All hydrochars exhibited type IV isotherms of IUPAC classification (Alothman, 2012), which are related to mesoporous adsorbents (e.g., many oxide gels, industrial adsorbents, and mesoporous molecular sieves). A typical feature of Type IV isotherms is a terminal saturation plateau of variable length (sometimes reduced to a mere inflection point). Although O-EFB280h2 was assigned to type IV, it also showed the large hysteresis loop associated with the large surface area, as shown in **Table 3**. Furthermore, these hysteresis loops were aligned with de Boer's classification of hysteresis (Liu *et al*., 2021) in the H3 type with slit-shaped pores (the isotherms revealing the H3 type showed unlimited adsorption at high P/Po, which is observed in non-rigid aggregates becomes). from platelet-shaped particles).

DOI: https://doi.org/10.17509/ijost.v9i3.74551
p- ISSN 2528-1410 e- ISSN 2527-8045

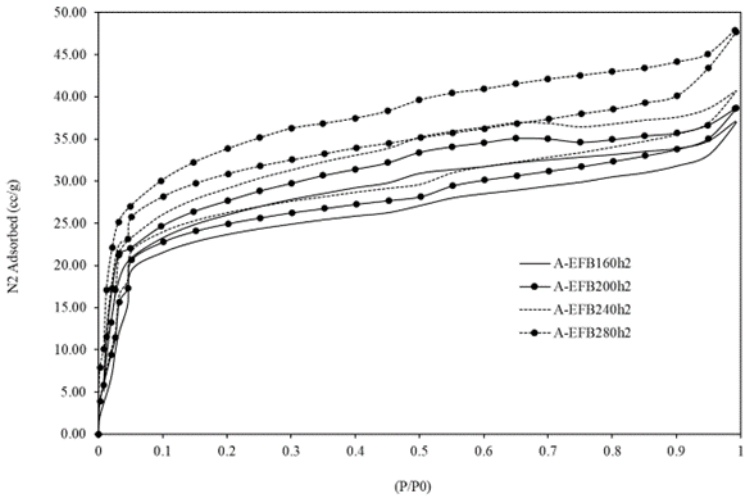

Figure 3. N_2 adsorption isotherm of hydrochar activated by H_2SO_4**.**

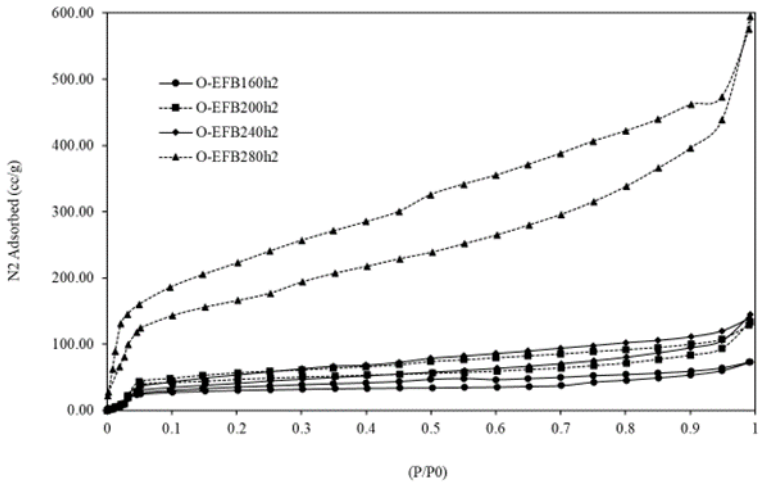

Figure 4. N_2 adsorption isotherm of hydrochar activated by H_2O_2.

The N_2 adsorption data were evaluated for the porosity of hydrochar such as surface area, average pore size, and total pore volume via the Brunauer–Emmett–Teller (BET) model. The results are presented in **Table 3**. Previous studies reported that hydrochars prepared from several materials via HTC have surface areas ranging from 2.09–21.00 m^2/g (Wang *et al.*, 2022). Although H_2SO_4 has been used as an activator in the preparation of hydrochar from bamboo via HTC, it did not increase the surface area because of the hardness of the bamboo structure. The bamboo hydrochar exhibited a surface area of 6.00 m^2/g (Zhang *et al.*, 2021). Following our previous study, the hydrochar in the conventional HTC process under the same conditions in the temperature range of 160–280 °C without using an activator showed surface areas in the range of 11.91–78.03 m^2/g (**Table 3**) (Sisuthog *et al.*, 2022).

In this study, the use of H_2SO_4 in the HTC process produced hydrochars with increased surface areas ranging from 76–99 m^2/g. Remarkably, the hydrochar produced via the H_2O_2-assisted HTC process at 280 °C exhibited an ultra-high surface area of 479.19 m^2/g and a deep pore volume of 0.727 cm^3/g, which were significantly higher than those of the conventional hydrochars (Roman *et al.*, 2013). The extremely high porosity of this hydrochar may be because of the occurrence of decarboxylation during the HTC process catalyzed by H_2O_2 at 280 °C. The peroxide group of H_2O_2 is an oxidizing group that affects the unstable carbon

DOI: https://doi.org/10.17509/ijost.v9i3.74551
p- ISSN 2528-1410 e- ISSN 2527-8045

structure of hydrochar, causing it to decompose. The results of the ultimate analysis (**Table 1**) showed that the carbon content of the hydrochar treated with H_2O_2 was lower than that of the hydrochar treated with H_2SO_4 under the same conditions. The increase in the surface area was caused by a partial decrease in the carbon content, which also increased the average pore volume. This was exhibited by the O-EFB280h2 sample (**Table 3**). The average pore diameters of the hydrochars obtained from the HTC process without an activator were in the range of 4.88–15.10 nm (Sisuthog *et al*., 2022). The use of activators in the HTC process significantly decreased the pore diameter to the range of 3.06–3.90 nm. H_2O_2 had a greater effect on the total pore volume than H_2SO_4 because of its strong reaction with the peroxide group. All as-prepared hydrochars exhibited a mesoporous structure suitable for use in the adsorption process.

Table 3. Textural properties of hydrochars prepared under various conditions.

Samples	S_{BET} (m^2/g)	Total pore volume (cm^3/g)	Average pore diameter (nm)
EFBs[a]	11.21	0.033	15.84
EFB160h2[a]	42.20	0.130	12.21
EFB200h2[a]	30.82	0.120	15.10
EFB240h2[a]	11.91	0.030	10.89
EFB280h2[a]	78.03	0.100	4.88
A-EFB160h2	76.10	0.023	3.82
A-EFB200h2	93.65	0.011	3.06
A-EFB240h2	84.31	0.026	3.32
A-EFB280h2	99.14	0.028	3.06
O-EFB160h2	63.75	0.073	3.90
O-EFB200h2	106.32	0.146	3.06
O-EFB240h2	115.30	0.176	3.42
O-EFB280h2	479.19	0.727	3.06

Note: [a] data in the literature (Sisuthog *et al*., 2022)

The occurrence of the decarboxylation reaction at temperatures higher than 240 °C using H_2O_2 as an activator is responsible for the extremely high porosity of the O-EFB280h2 sample. By oxidizing the peroxide group, cellulose, which is a major component of EFBs, is degraded to the carboxylic group, which is then converted to an alkane (liquid phase) and CO_2 (gaseous phase). The mass loss of the EFB structure affects the increase in porosity (Kulikowska *et al*., 2013), resulting in a high surface area. **Figure 5** illustrates the reaction pathway of the decarboxylation process.

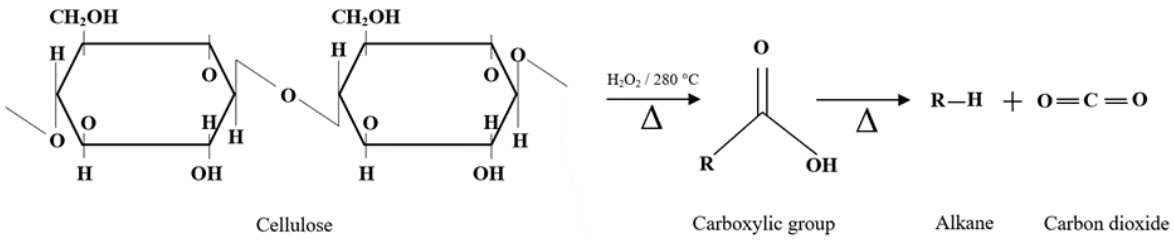

Figure 5. Proposed reaction pathway for the decarboxylation of EFBs.

The O-EFB280h2 hydrochar prepared in this study exhibited a significantly higher surface area than the other hydrochars prepared in previous studies, as shown in **Table 4**. This indicates that the hydrochar may not need to activate the process and uses less (Roman *et al*., 2013) energy to increase the surface area.

DOI: https://doi.org/10.17509/ijost.v9i3.74551
p- ISSN 2528-1410 e- ISSN 2527-8045

Table 4. BET surface area of the hydrochars obtained from different starting materials.

Biomass/starting material	Activators	BET surface area (m^2/g)	Reference
Oak leaf	$C_6H_{10}O_8$	15.50	(Titirici *et al*., 2007)
Pinecone	$C_6H_{10}O_8$	34.00	(Titirici *et al*., 2007)
Hazelnut shell	$C_6H_{10}O_8$	60.00	(Titirici *et al*., 2007)
Bamboo	HCl	10.96	(Zhang *et al*., 2021)
Bamboo	H_2SO_4	6.06	(Zhang *et al*., 2021)
Bamboo	HNO_3	15.12	(Zhang *et al*., 2021)
Peanut hull	H_2O_2	115.80	(Xue *et al*., 2012)
EFBs	H_2SO_4	99.14	This study
EFBs	H_2O_2	479.19	This study

SEM was employed at a magnification of 3,000× to investigate the surface morphology of the as-prepared materials (**Figure 6**). The surface of the EFBs that served as the raw material revealed a smooth and even texture (**Figure 6a**), which is a characteristic of lignocellulosic materials. A significant degradation of the structure of the EFBs (A-EFB280h2) was observed after the HTC process catalyzed by H_2SO_4 (**Figure 6b**). This resulted in the formation of a hydrochar characterized by a rougher exterior, with tiny particles adhering to it. In contrast, the hydrochar (O-EFB280h2) produced from the HTC process catalyzed by H_2O_2 showed a significant alteration in surface topography and a prominent rectangular morphology (**Figure 6c**). It appeared that H_2SO_4 eroded the pores, particularly the exterior of the hydrochar, whereas H_2O_2 with the peroxide functional group reacted strongly with the hydrochar surface, thus generating deeper pores.

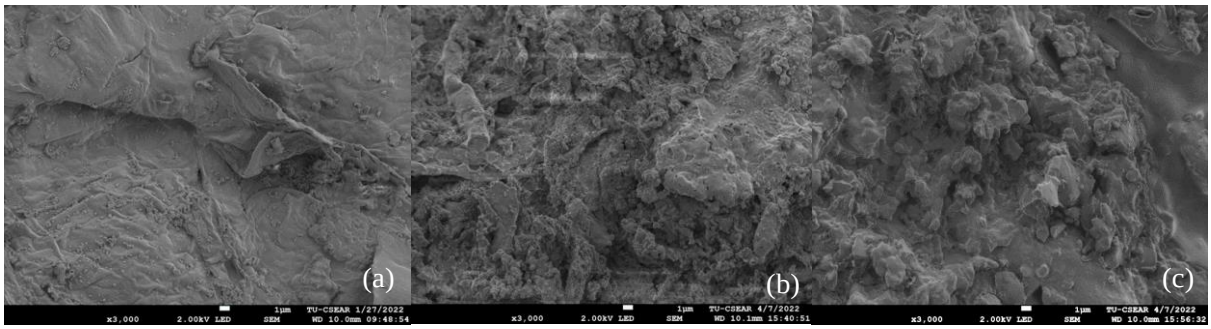

Figure 6. SEM images of samples: (a) EFB, (b) A-EFB280h2, and (c) O-EFB280h2 samples.

3.3. FT-IR Spectra

Figure 7 shows the FT-IR spectra of the EFBs and hydrochars prepared under various HTC operating parameters. Different operating conditions affected the presence of chemical functional groups. The topmost FT-IR spectra (indicated in black) shown in **Figures 7(a)** and **7(b)** are of the raw EFBs. A strong band corresponding to the hydroxyl group (O-H stretching) appeared in the range of 3,200–3,400 cm^{-1}. Bands corresponding to the aliphatic group (C-H stretching) were observed in the range of 2,840–2,900 cm^{-1} and those corresponding to the stretching vibrations of the carbonyl (C=O) group were observed in the range of 1,705–1,725 cm^{-1}. A very strong band corresponding to the C-O stretching vibration of the ether group was observed in the range of 1,000–1,100 cm^{-1}. These results indicate that the EFBs are lignocellulosic materials.

DOI: https://doi.org/10.17509/ijost.v9i3.74551
p- ISSN 2528-1410 e- ISSN 2527-8045

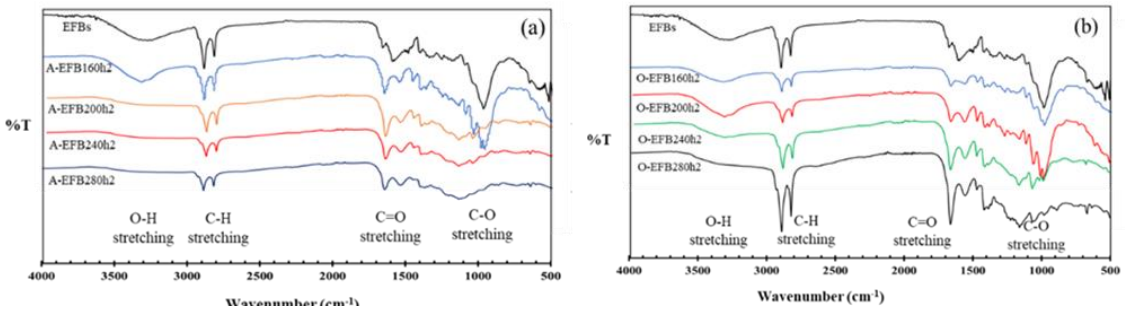

Figure 7. FT-IR spectra of the EFBs and biochars activated via the (a) H_2SO_4 and (b) H_2O_2.

As the operating temperature of the HTC process catalyzed by the H_2O_2 and H_2SO_4 activators increased, the bands corresponding to the stretching vibrations of the hydroxyl (3,200–3,400 cm^{-1}) and ether (1,000–1,100 cm^{-1}) groups in the hydrochar samples disappeared, as shown in **Figures 7a** and **7b**, respectively. The intensities of the C-H bands (2,840–2,900 cm^{-1}) and the C=O stretching peaks (1,705–1,725 cm^{-1}) in the FT-IR spectra of the hydrochars prepared via the H_2O_2-activated HTC process increased with increasing operating temperature. In contrast, the intensities of the C-H (2,840–,900 cm^{-1}) and C=O (1,705–1,725 cm^{-1}) stretching peaks in the FT-IR spectra of the hydrochars prepared using the H_2SO_4-activated HTC process in each condition did not change. Thus, H_2SO_4 did not affect the functional groups of the EFBs. However, a greater number of OFGs were obtained when H_2O_2 was used, as evidenced by the increase in the intensity of the C=O stretching peak with increasing operating temperature. This is advantageous for the hydrochars because the number of OFGs is related to the increase in the surface area following the activation process (Mamimin *et al*., 2021). The O-EFB280h2 sample, which possessed a high surface area of 479.19 m^2/g and exhibited prominent C-H and C=O stretching bands, revealed the advantage of using H_2O_2 during the HTC process. These results indicate that the waste EFBs have the potential to be developed into valuable materials. Hydrochars derived from them exhibited high surface areas of up to 479.19 m^2/g. This makes them suitable for further applications as absorbent materials, such as oil-absorbing biomass materials (Yang *et al*., 2021). Additionally, because of their OFGs, they can also be used as activators, which accelerate the reactions (Bhoi *et al*., 2020).

4. CONCLUSION

In this study, the HTC process catalyzed by a hydrolytic agent (H_2O_2 or H_2SO_4) was used to convert EFBs into hydrochars, which displayed remarkable properties, in a single step. The fixed carbon and carbon contents increased with increasing HTC temperature. The hydrochar produced using the HTC process catalyzed by H_2SO_4 at 280 °C for 2 h exhibited the highest carbon and fixed carbon contents of 72.65 and 38.35 wt.%, respectively. The H_2O_2-assisted HTC process produced a hydrochar (O-EFB280h2) with the highest surface area (479.19 m^2/g) and pore volume (0.727 cm^3/g) under the same conditions. All the biochars containing the functional groups C-H, C=O, and C-O were oxygenated materials. Based on their physical and chemical properties, they can be converted into hydrochars with a high surface area in a single step.

5. ACKNOWLEDGMENT

This research was supported by the Science, Research and Innovation Promotion Fund, Thailand Science Research and Innovation (TSRI), through Rajamangala University of

DOI: https://doi.org/10.17509/ijost.v9i3.74551
p- ISSN 2528-1410 e- ISSN 2527-8045

Technology Thanyaburi (FRB66E0705E and FRB66E0706E.1) (grant number FRB660012/0168). Thailand Institute of Scientific and Technological Research (TISTR) on Project No. 78136 and Suksomboon Palm Oil Co., Ltd. were supplied with instruments and raw materials.

6. AUTHORS' NOTE

The authors declare that there is no conflict of interest regarding the publication of this article. The authors confirmed that the paper was free of plagiarism.

7. REFERENCES

Alothman, Z. (2012). A review: Fundamental aspects of silicate mesoporous materials. *Materials*, *5*, 2874–2902.

Ameen, M., Zamri, N. M., May, S. T., Azizan, M. T., Aqsha, A., Sabzoi, N., and Sher, F. (2022). Effect of acid catalysts on hydrothermal carbonization of Malaysian oil palm residues (leaves, fronds, and shells) for hydrochar production. *Biomass Conversion and Biorefinery*, *12*, 103–114.

Bhoi, P. R., Ouedraogo, A. S., Soloiu, V., and Quirino, R. (2020). Recent advances on catalysts for improving hydrocarbon compounds in bio-oil of biomass catalytic pyrolysis. *Renewable and Sustainable Energy Reviews*, *121*, 109676.

Cebi, D., Celiktas, M. S., and Sarptas, H. (2022). A review on sewage sludge valorization via hydrothermal carbonization and applications for circular economy. *Circular Economy and Sustainability*, *2*(4), 1345–1367.

Duy Nguyen, H., Nguyen Tran, H., Chao, H.-P., and Lin, C.-C. (2019). Activated carbons derived from teak sawdust-hydrochars for efficient removal of methylene blue, copper, and cadmium from aqueous solution. *Water*, *11*(12), 2581.

Fakkaew, K., Koottatep, T., and Polprasert, C. (2015). Effects of hydrolysis and carbonization reactions on hydrochar production. *Bioresource Technology*, *192*, 328–334.

Jain, A., Balasubramanian, R., and Srinivasan, M. P. (2015). Production of high surface area mesoporous activated carbons from waste biomass using hydrogen peroxide-mediated hydrothermal treatment for adsorption applications. *Chemical Engineering Journal*, *273*, 622–629.

Kambo, H. S., and Dutta, A. (2015). A comparative review of biochar and hydrochar in terms of production, physico-chemical properties and applications. *Renewable and Sustainable Energy Reviews*, *45*, 359–378.

Khoshbouy, R., Takahashi, F., and Yoshikawa, K. (2019). Preparation of high surface area sludge-based activated hydrochar via hydrothermal carbonization and application in the removal of basic dye. *Environmental Research*, *175*, 457–467.

Kulikowska, A. A., Wasiak, I., and Ciach, T. (2013). Carboxymethyl cellulose oxidation to form aldehyde groups. *Challenges of Modern Technology*, *4*(2), 1-9.

Li, F., Zimmerman, A. R., Hu, X., Yu, Z., Huang, J., and Gao, B. (2020). One-pot synthesis and characterization of engineered hydrochar by hydrothermal carbonization of biomass with $ZnCl_2$. *Chemosphere*, *254*, 126866.

DOI: https://doi.org/10.17509/ijost.v9i3.74551
p- ISSN 2528-1410 e- ISSN 2527-8045

Li, R., and Shahbazi, A. (2015). A review of hydrothermal carbonization of carbohydrates for carbon spheres preparation. *Trends in Renewable Energy*, *1*(1), 43–56.

Liu, K., Zakharova, N., Adeyilola, A., and Zeng, L. (2021). Experimental study on the pore shape damage of shale samples during the crushing process. *Energy and Fuels*, *35*(3), 2183–2191.

Malaika, A., Heinrich, M., Goscianska, J., and Kozłowski, M. (2020). Synergistic effect of functional groups in carbonaceous spheres on the formation of fuel enhancers from glycerol. *Fuel*, *280*, 118523.

Mamimin, C., Chanthong, S., Leamdum, C., Sompong, O., and Prasertsan, P. (2021). Improvement of empty palm fruit bunches biodegradability and biogas production by integrating the straw mushroom cultivation as a pretreatment in the solid-state anaerobic digestion. *Bioresource Technology*, *319*, 124227.

Nizamuddin, S., Baloch, H. A., Griffin, G. J., Mubarak, N. M., Bhutto, A. W., Abro, R., Mazari, S. A., and Ali, B. S. (2017). An overview of effect of process parameters on hydrothermal carbonization of biomass. *Renewable and Sustainable Energy Reviews*, *73*, 1289–1299.

Puccini, M., Stefanelli, E., Hiltz, M., Seggiani, M., and Vitolo, S. (2017). Activated carbon from hydrochar produced by hydrothermal carbonization of wastes. *Chemical Engineering Transactions*, *57*, 169–174.

Rohimi, N. F., Yaakob, M. N. A., Roslan, R., Salim, N., Mustapha, S. N. H., Rahim, M. H. A., Chia, C.-H., and Zakaria, S. (2022). Structural and thermal analysis of bio-based polybenzoxazine derived from liquefied empty fruit bunch (EFB) via solventless method. *Materials Today: Proceedings*, *51*, 1367–1371.

Roman, S., Nabais, J. M. V., Ledesma, B., González, J. F., Laginhas, C., and Titirici, M. M. (2013). Production of low-cost adsorbents with tunable surface chemistry by conjunction of hydrothermal carbonization and activation processes. *Microporous and Mesoporous Materials*, *165*, 127–133.

Sisuthog, W., Attanatho, L., and Chaiya, C. (2022). Conversion of empty fruit bunches (EFBs) by hydrothermal carbonization towards hydrochar production. *Energy Reports*, *8*, 242–248.

Soha, M., Khaerudini, D. S., Chew, J. J., and Sunarso, J. (2021). Wet torrefaction of empty fruit bunches (EFB) and oil palm trunks (OPT): Efects of process parameters on their physicochemical and structural properties. *South African Journal of Chemical Engineering*, *35*(1), 126–136.

Titirici, M. M., Thomas, A., Yu, S. H., Müller, J. O., and Antonietti, M. (2007). A direct synthesis of mesoporous carbons with bicontinuous pore morphology from crude plant material by hydrothermal carbonization. *Chemistry of Materials*, *19*(17), 4205–4212.

Wadchasit, P., Suksong, W., Sompong, O., and Nuithitikul, K. (2021). Development of a novel reactor for simultaneous production of biogas from oil-palm empty fruit bunches (EFB) and palm oil mill effluents (POME). *Journal of Environmental Chemical Engineering*, *9*(3), 105209.

DOI: https://doi.org/10.17509/ijost.v9i3.74551
p- ISSN 2528-1410 e- ISSN 2527-8045

Wang, X., Shen, Y., Liu, X., Ma, T., Wu, J., and Qi, G. (2022). Fly ash and H_2O_2 assisted hydrothermal carbonization for improving the nitrogen and sulphur removal from sewage sludge. *Chemosphere*, *290*, 133209.

Wu, S., Wang, Q., Cui, D., Sun, H., Yin, H., Xu, F., and Wang, Z. (2023a). Evaluation of fuel properties and combustion behaviour of hydrochar derived from hydrothermal carbonisation of agricultural wastes. *Journal of the Energy Institute*, *108*, 101209.

Wu, S., Wang, Q., Cui, D., Wang, X., Wu, D., Bai, J., Xu, F., Wang, Z., and Zhang, J. (2023b). Analysis of fuel properties of hydrochar derived from food waste and biomass: evaluating varied mixing techniques pre/post-hydrothermal carbonization. *Journal of Cleaner Production*, *430*, 139660.

Xue, Y., Gao, B., Yao, Y., Inyang, M., Zhang, M., Zimmerman, A. R., and Ro, K. S. (2012). Hydrogen peroxide modification enhances the ability of biochar (hydrochar) produced from hydrothermal carbonization of peanut hull to remove aqueous heavy metals: Batch and column tests. *Chemical Engineering Journal*, *200*, 673–680.

Yan, M., Hantoko, D., Susanto, H., Ardy, A., Waluyo, J., Weng, Z., and Lin, J. (2019). Hydrothermal treatment of empty fruit bunch and its pyrolysis characteristics. *Biomass Conversion and Biorefinery*, *9*, 709–717.

Yang, Q., Sun, Y., Sun, W., Qin, Z., Liu, H., Ma, Y., and Wang, X. (2021). Cellulose derived biochar: Preparation, characterization and Benzo [a] pyrene adsorption capacity. *Grain and Oil Science and Technology*, *4*(4), 182–190.

Zhang, S., Sheng, K., Yan, W., Liu, J., Shuang, E., Yang, M., and Zhang, X. (2021). Bamboo derived hydrochar microspheres fabricated by acid-assisted hydrothermal carbonization. *Chemosphere*, *263*, 128093.

Zhu, Y., Xie, Q., Zhu, R., Lv, Y., Xi, Y., Zhu, J., and Fan, J. (2022). Hydrothermal carbons/ferrihydrite heterogeneous Fenton catalysts with low H_2O_2 consumption and the effect of graphitization degrees. *Chemosphere*, *287*, 131933.

DOI: https://doi.org/10.17509/ijost.v9i3.74551
p- ISSN 2528-1410 e- ISSN 2527-8045